JPET Fast Forward. Published on May 11, 2006 as DOI: 10.1124/jpet.106.102616
This article has not been copyedited and formatted. The final version may differ from this version.

JPET #102616

HEPATOBILIARY DISPOSITION OF A DRUG/METABOLITE PAIR: COMPREHENSIVE PHARMACOKINETIC MODELING IN SANDWICH-CULTURED RAT HEPATOCYTES

Ryan Z. Turncliff, Keith A. Hoffmaster, J. Cory Kalvass,
Gary M. Pollack, Kim L.R. Brouwer

School of Pharmacy, University of North Carolina, Chapel Hill, North Carolina

Running Title: Disposition of a drug/metabolite pair in SC-rat hepatocytes

Corresponding Author:

Dr. Kim L.R. Brouwer
School of Pharmacy
Kerr Hall, CB #7360
University of North Carolina at Chapel Hill
Chapel Hill, NC 27599-7360

E-mail: **kbrouwer@unc.edu**

Telephone: 919-962-7030

Number of Text Pages: 17

Number of Tables: 3

Number of Figures: 6

Number of References: 35

Number of Words:

Abstract: 238

Introduction: 780

Discussion: 1611

List of Abbreviations:

TER, Terfenadine; FEX, fexofenadine; AZA, azacyclonol; DEX, Dexamethasone; HBSS, Hank's balanced salt solution; SC, Sandwich-cultured; BC, bile-canaliculi.

Section: Absorption, Distribution, Metabolism & Excretion

Abstract.

The hepatobiliary disposition of xenobiotics may involve passive and/or active uptake, metabolism by cytochromes P450, and excretion of the parent compound and/or metabolite(s) into bile. While *in vitro* systems have been used to evaluate these individual processes discretely, mechanistic *in vitro* studies of the sequential processes of uptake, metabolism, and biliary or basolateral excretion are limited. The current studies utilized sandwich-cultured (SC) rat hepatocytes combined with a comprehensive pharmacokinetic modeling approach to investigate the hepatobiliary disposition of terfenadine and fexofenadine, a model drug/metabolite pair. The metabolism of terfenadine and the biliary excretion of terfenadine and fexofenadine were determined in control and dexamethasone-treated SC rat hepatocytes. Dexamethasone (DEX) treatment increased the formation rates of the terfenadine metabolites azacyclonol and fexofenadine ~20-fold and 2-fold, respectively. The biliary excretion index (BEI) of fexofenadine generated by terfenadine metabolism was not significantly different from the BEI of preformed fexofenadine (15±2% *vs.* 19±2%, respectively). Pharmacokinetic modeling revealed that the rate constant for hepatocyte uptake was faster for terfenadine compared to preformed fexofenadine [2.5 hr^{-1}*vs.* 0.08 hr^{-1}, respectively], while the biliary excretion rate constant for preformed fexofenadine exceeded that of terfenadine [0.44 hr^{-1} vs. 0.039 hr^{-1}, respectively]. Interestingly, the rate constant for basolateral excretion of terfenadine and fexofenadine were comparable [3.2 hr^{-1} vs. 1.9 hr^{-1}, respectively], and increased only slightly with DEX treatment. These studies demonstrate the utility of the SC hepatocyte model, coupled with pharmacokinetic modeling, to evaluate the hepatobiliary disposition of generated metabolites.

Biliary clearance is a predominant route of elimination for many compounds including bile salts, organic anions and organic cations. In recent years, the mechanisms involved in the hepatic uptake, as well as the sinusoidal and canalicular excretion, of many substances have been elucidated. Following transport into the hepatocyte, many compounds undergo Phase I and/or Phase II metabolism prior to excretion into bile (by canalicular transport proteins) or sinusoidal blood (by basolateral transport proteins). Pang and co-workers have clearly established that, in some cases, the hepatic disposition of an administered, preformed metabolite may be very different from a metabolite generated in the intact organ (Tirona and Pang, 1996; Pang et al., 1984). However, differences in disposition of a generated vs. preformed metabolite are by no means assured, and must be demonstrated on a case-by-case basis.

Recent advances in molecular biology have allowed the mechanistic investigation of discrete transport or metabolic processes in isolation through administration of parent drug or metabolite to a variety of transfected, cell-based expression systems (Wrighton et al., 1995; Mizuno et al. 2003). Cummins et al. (2004) explored the interplay between transport and metabolism of midazolam and sirolimus in Caco-2 cells transfected with CYP3A4, while Sasaki et al. (2004) utilized double-transfected (OATP2/MRP2) MDCK cells to explore the potential rate-limiting step in the biliary disposition of a variety of substrates. The ability to quantify the impact of both hepatic transport and metabolism of drug candidates in a single *in vitro* system would offer significant advantages over existing methodologies.

Primary rat hepatocytes have been used to explore both hepatic metabolism and transport processes (Li, 1997; Liu et al., 1999a;, Kostrubsky et al., 2003). Rat

hepatocytes cultured between two layers of gelled collagen in a sandwich configuration form extensive, functional bile canalicular networks (LeCluyse et al., 1994). Moreover, an *in vitro/in vivo* correlation of biliary clearance for non-metabolically labile substrates such as methotrexate, [D-pen^{2,5}]enkephalin, and taurocholate (Liu et al., 1999a) has been established in SC rat hepatocytes. When cultured over time, the expression of some Phase I metabolizing enzymes in rat hepatocytes is diminished relative to the *in vivo* condition. However, dexamethasone (DEX) induces cytochrome P450 CYP3A1/2 in primary rat hepatocytes, and is useful in maintaining CYP3A1/2 activity in SC rat hepatocytes (LeCluyse et al., 1996; Li, 1997). The function and expression of Oatp1, Oatp2 and Mdr1a/b in SC rat hepatocytes has been demonstrated (Annaert et al., 2001; Hoffmaster et al., 2004), and the effect of DEX treatment on the expression and function of these and other transport proteins (eg. Bsep, Mrp2, Ntcp) in SC rat hepatocytes also has been reported (Turncliff et al., 2004).

The metabolic and transport processes that mediate the hepatobiliary disposition of terfenadine, and the terfenadine carboxylate metabolite fexofenadine, have been described (Jurima-Romet et al., 1995; Cvetkovic et al., 1999). The metabolism of terfenadine (Figure 1) by cytochrome P450s, including the role of CYP3A in the formation of the azacyclonol metabolite of terfenadine, has been well documented in microsomes and S9 fractions (Yun et al., 1993; Jurima-Romet et al., 1994; Raeissi et al., 1999). Hait et al. (1993) first suggested the involvement of P-gp in terfenadine transport. Oatp1a1 and Oatp1a4 likely mediate the hepatic uptake of fexofenadine in rat liver (Cvetkovic et al., 1999). Fexofenadine is a known Mdr1a/b substrate (Cvetkovic et al., 1999). However, recent work by Tahara et al. (2005) suggests that fexofenadine may be

a substrate for multiple, species-specific transport mechanisms. These observations further support the need for an *in vitro* model representative of *in vivo* hepatic transport and metabolism.

Pharmacokinetic modeling of *in vivo* or *in vitro* data can provide additional insight into the disposition of drugs and drug candidates. For example, modeling and simulation of verapamil disposition in Caco-2 cells suggested a nonlinear relationship between the extent of drug metabolism and the extent of drug transport (Johnson et al., 2003). Utilization of strategies to predict the extent of biliary clearance of parent compound and/or metabolite, and to identify rate-limiting steps in hepatobiliary disposition for the purpose of predicting potential sites of drug interactions is becoming increasingly important in the drug development process.

In the current studies, terfenadine and fexofenadine were selected as a model drug/metabolite pair to examine differences in the hepatobiliary disposition of a metabolite when generated *in vitro* vs. administered pre-formed in SC rat hepatocytes. Pharmacokinetic modeling of data was utilized to elucidate relative rates of transport and metabolic processes for terfenadine, fexofenadine, and azacyclonol. The hepatobiliary disposition of pre-formed fexofenadine was compared to fexofenadine generated by metabolism of terfenadine. This represents the first report using an *in vitro* model to examine the kinetics of hepatic uptake and biliary excretion of a drug/metabolite pair, including both preformed and generated metabolite.

Methods

Chemicals. Collagenase (type 1, class 1) was obtained from Worthington Biochemical Corporation (Freehold, NJ). Dulbecco's modified Eagle's medium (DMEM) and insulin were purchased from Invitrogen/GIBCO (Carlsbad, CA). ITS^{+TM} culture supplement and rat tail collagen (type I) were purchased from BD Biosciences (Bedford, MA). DMEM (10x), penicillin-streptomycin solution, fetal bovine serum (FBS), taurocholic acid (TC), dexamethasone (DEX), Triton X-100, soybean trypsin inhibitor, terfenadine, fexofenadine and loperamide were purchased from Sigma-Aldrich. Azacyclonol (α,α,-diphenyl-4-piperidine-methanol) was purchased from Arcos Organics (Fisher Chemical, Pittsburgh, PA). All other chemicals and reagents were of analytical grade and were readily available from commercial sources.

Animals. Male Wistar rats (270-325 g) obtained from Charles River Laboratories (Raleigh, NC) were used for hepatocyte isolation from whole liver. Animals had free access to water and food prior to surgery. All animal procedures were compliant with the guidelines of the University of North Carolina Institutional Animal Care and Use Committee.

Isolation and In Vitro Culture of Primary Rat Hepatocytes. Hepatocytes were isolated from male Wistar rats using a collagenase perfusion, and were cultured as described previously (Liu et al., 1999b); hepatocyte viability was >85% as determined by trypan blue exclusion. Briefly, hepatocytes were plated at a density of ~3.0 x 10^6 cells/dish in 60-mm dishes previously coated with 0.2 ml rat tail collagen type I solution (1.5 mg/ml, pH 7.4). After 24 hr (Day 1), medium was aspirated and cells were overlaid with 200 µl of rat tail collagen type I solution (1.5 mg/ml, pH 7.4) to achieve a sandwich

configuration. Subsequently, medium (DMEM supplemented with 1 % ITS+, penicillin/streptomycin, L-glutamine, non-essential amino acids, and 0.1 μM DEX) was changed every 24 hr until metabolism and/or biliary excretion experiments were performed.

SC Rat Hepatocyte DEX Treatment. DEX (100 μM) or vehicle (DMSO) was added to the culture medium beginning on Day 2. The final concentration of DMSO in culture medium was <0.1%. SC rat hepatocytes were treated with DEX or vehicle for 48 hr.

Metabolism of Terfenadine and Fexofenadine in SC Rat Hepatocytes. On Day 4, SC rat hepatocytes were rinsed with warm DMEM prior to addition of 3 ml Hank's balanced salt solution (HBSS) (for early time points) or DMEM (for long time points) containing terfenadine (5 μM) or fexofenadine (5 μM). HBSS samples (1 ml) were obtained at 0, 0.25, 0.5, and 1 hr, while DMEM samples (1 ml) were obtained at 2, 4, 8 and 12 hr. All samples were stored at -20^0C until analysis. Three dishes of hepatocytes were sampled at each time point. Following removal of the remaining incubation medium and rinsing with ice-cold HBSS (3 x 3 ml), methanol (1 ml) was added to each culture dish and the cells were scraped off of the dishes and stored at -20^0C until analysis.

Biliary Excretion of Terfenadine and Fexofenadine. The biliary excretion index (BEI) was calculated using B-CLEAR® technology (Qualyst, Inc., Raleigh, NC) by dividing the difference in substrate accumulation between standard HBSS (cellular plus canalicular accumulation) and Ca^{2+}-free HBSS (cellular accumulation) by the accumulation in standard HBSS (Liu et al., 1999b). Briefly, Day 4 SC rat hepatocytes were rinsed twice with 3 ml warm standard HBSS [cells+bile canaliculi (BC)] or Ca^{2+}-free HBSS [cells] and incubated with 3 ml of the same buffer for 10 min at 37^0C. SC rat hepatocytes were

incubated with 3 ml of terfenadine (5 μM) or preformed fexofenadine (5 μM) for 0.25, 0.5 and 1 hr in standard HBSS. At each time point, an HBSS sample (1 ml) was removed for analysis; the remainder was aspirated. Subsequently, SC rat hepatocytes were rinsed vigorously 3 times with 3 ml ice-cold HBSS. Hepatocytes were lysed with 1 ml of methanol. All dishes were scraped and lysates were stored at -20^0C until analysis by HPLC.

Non-specific Binding and Protein Determination. Accumulation data were corrected for nonspecific binding of the relevant substrate to gelled-collagen coated hepatocyte-free culture dishes at each time point. All data were normalized to the average protein content in ~10 dishes/experiment (lysed with Triton-X 100) as determined with a commercially available kit (BCA Protein Assay, Pierce Chemical Co., Rockford, IL), based on instructions provided by the manufacturer. Bovine serum albumin was used as the standard (supplied with the BCA kit).

HPLC Analysis. The amount of terfenadine and fexofenadine in both incubation medium and cell lysates from SC rat hepatocyte accumulation experiments was determined by HPLC with fluorescence detection using a method modified from Coutant et al. (1991). Briefly, following centrifugation at 3000*g* to pellet precipitated protein, 50 μl supernatant was injected onto a 250 x 4.6 mm BDS Cyano-Hypersil® column (Thermo Hypersil-Keystone, Bellafonte, PA) using a Shimadzu SCL-10A/SIL-10A controller/autosampler combination (Shimadzu, Columbia, MD). Mobile phase consisted of 12 mM ammonium acetate, acetonitrile and methanol [52:12:36; pH 3.0, adjusted with HCl] and was delivered at a flow rate of 1 ml/min by a Shimadzu LC-10Advp pump; run times were 30 min. The fluorescence of the column eluent was monitored with a Jasco (Easton, MD)

FP-920 fluorescence detector (λ ex: 230 nm; λ em: 280 nm). Standard curves for terfenadine and fexofenadine were linear from 25 – 1000 ng/ml and 25 – 500 ng/ml, respectively.

LC/MS/MS Analysis. Due to limitated sensitivity of the HPLC method, concentrations of azacyclonol were determined by LC/MS/MS in a sub-set of samples. Concentrations of terfenadine and fexofenadine also were quantitated in these samples for comparison to concentrations determined by HPLC. Samples were prepared as described above. An aliquot of supernatant was transferred to an HPLC vial to which 250 µl of methanol containing internal standard (20 ng/ml of loperamide) was added; samples were mixed by vortex for 30 seconds. Samples were injected (Agilent 1100 96-well plate autosampler) onto a 2.0 x 30 mm, 4 µM Synergi Max-RP column (Phenomenex, Torrance, CA) maintained at room temperature with a run time of 4 min. Analytes were eluted with a high-pressure linear gradient program consisting of 10 mM ammonium acetate, pH 6.8 (A); methanol (B) delivered by an Agilent 1100 series binary pump (flow rate = 0.75 mL/min) as follows: 20% B to 95% B over 2 min, hold 95% B for 1 min, returned rapidly to 20% B over 0.1 min. The system was allowed to re-equilibrate for 1 min. The entire column effluent was diverted from the Turbo Ionspray probe of an API-4000 triple quadrupole mass spectrometer (Applied Biosystems; Foster City, CA) for the first and last min. terfenadine, fexofenadine, azacyclonol, and loperamide were detected using selected reaction monitoring. The lower and upper limits of quantification of terfenadine, azacyclonol and fexofenadine were 1 and 100 ng/ml, respectively. Terfenadine and fexofenadine concentrations determined by LC/MS/MS were in good agreement with results from the HPLC assay.

JPET Fast Forward. Published on May 11, 2006 as DOI: 10.1124/jpet.106.102616
This article has not been copyedited and formatted. The final version may differ from this version.

Data Analysis. The amount of terfenadine, fexofenadine, and azacyclonol in medium and cell lysates was determined in triplicate from three individual livers. The BEI (%) of terfenadine, generated fexofenadine and preformed fexofenadine was determined as:

$$BEI(\%) = \left(\frac{Accumulation_{[cells + BC]} - Accumulation_{[cells]}}{Accumulation_{[cells + BC]}} \right) \bullet 100$$

BEI was calculated as a mean of BEI values from the individual livers and is expressed as mean ± SEM. The *in vitro* biliary clearance ($Cl_{B\ in\ vitro}$) of terfenadine and preformed fexofenadine was calculated as previously described (Liu et al. 1999a) with modifications as described in Appendix I . Area under the curve (AUC) values were calculated by either the linear or log-linear trapezoidal methods as noted in Appendix I.

Pharmacokinetic Modeling. Pooled (n=3) terfenadine, generated fexofenadine and preformed fexofenadine amount (pmol/mg protein) data were used in pharmacokinetic model development. A one-compartment model [bolus input, single first-order elimination rate constant] was used to describe the disappearance of terfenadine from the total SC rat hepatocyte incubation (medium+cell+BC). Data from control and DEX-treated SC rat hepatocyte experiments were truncated at 4 hr in the analysis of terfenadine disappearance; all time points were used in all subsequent models. Model schemes were selected following comparison of AIC values and visual inspection of the generated curves from a series of multi-compartment models. Differential equations listed in Appendix II, corresponding to the model schemes depicted in Figure 2, were solved simultaneously using WinNonlin version 3.2 (Pharsight Corporation, Mountain View, CA). A stepwise modeling approach was employed to isolate parameter estimates associated with the disposition of terfenadine, generated fexofenadine, generated azacyclonol, and preformed fexofenadine in control and DEX-treated SC rat hepatocytes.

Model 1 (Figure 2) was used to derive parameter estimates regarding the accumulation, metabolism and biliary excretion of terfenadine. Subsequently, the parameter estimates from Model 1 were fixed in Model 2 to generate parameter estimates pertaining to the sinusoidal efflux, sinusoidal uptake, and canalicular excretion of generated fexofenadine. Model 3 was used to estimate rate constants describing the accumulation, sinusoidal efflux and canalicular excretion of preformed fexofenadine. Simulation experiments were conducted to evaluate the capability of the estimated rate constants to describe the metabolism and biliary excretion of terfenadine and generated fexofenadine. Estimates of the rate constants associated with the disposition of terfenadine in Day 4 control SC rat hepatocytes generated in Models 1 and 3 were fixed in Model 2 to simulate the accumulation of terfenadine and formation of fexofenadine in cells+BC and cells in control and DEX-treated SC rat hepatocytes.

Statistical Analysis. Statistical differences in BEI or biliary clearance between control and DEX-treated Day 4 SC rat hepatocytes were determined by Students' *t* test (Table 1). Two-way ANOVA tables were constructed to compare the amount of substrate in medium and cells at selected time points in control *vs.* DEX-treated SC rat hepatocytes (Table 2); where appropriate, two-way ANOVA was followed by a Tukey test. The criterion for statistical significance was $P < 0.05$.

Results

Non-specific Binding of Terfenadine and Fexofenadine. The non-specific binding of both terfenadine and fexofenadine to gelled-collagen coated polystyrene culture dishes was <5 % of the initial mass, and therefore was assumed to be insignificant.

Metabolism and Biliary Excretion of Preformed Fexofenadine in SC Rat Hepatocytes. Cummulative recovery of preformed fexofenadine in Day 4 SC rat hepatocytes (medium+cell+BC) was >90% and was not significantly different between control and DEX-treated groups (data not shown). The accumulation of preformed fexofenadine in cells+BC *vs.* cells of control and DEX-treated SC rat hepatocytes is shown in Figure 3. The BEI and $Cl_{B\ in\ vitro}$ values for preformed fexofenadine were not significantly different between control and DEX-treated SC rat hepatocytes (Table 1).

Metabolism of Terfenadine and Biliary Excretion of Terfenadine and Generated Fexofenadine in Day 4 SC Rat Hepatocytes. The disappearance of terfenadine from medium, cellular accumulation of terfenadine, generation of azacyclonol, and the amount of generated fexofenadine in cells and medium in Day 4 control and DEX-treated SC rat hepatocytes is shown in Figure 4. The accumulation of terfenadine and the fexofenadine metabolite in cells+BC *vs.* cells of control and DEX-treated SC rat hepatocytes is shown in Figure 5. The BEI of terfenadine in control Day 4 SC rat hepatocytes was significantly higher compared to DEX-treated Day 4 SC rat hepatocytes; however, $Cl_{B\ in\ vitro}$ values were similar between the two groups (Table 1). At 1 hr, the BEI of generated fexofenadine was similar in control and DEX-treated Day 4 SC rat hepatocytes (Table 1).

Effect of DEX Treatment on the Metabolism of Terfenadine in Day 4 SC Rat Hepatocytes. Concentration-time profiles of terfenadine in control and DEX-treated Day 4 SC rat

JPET Fast Forward. Published on May 11, 2006 as DOI: 10.1124/jpet.106.102616
This article has not been copyedited and formatted. The final version may differ from this version.

hepatocytes are shown in Figure 6. A one-compartment model was employed to estimate the elimination rate constant for terfenadine (0-4 hr). The rate constant governing mono-exponential terfenadine loss from Day 4 SC rat hepatocytes (medium+cell) treated with DEX ($k = 1.04 \pm 0.2$ hr^{-1}; $t_{1/2} = 0.7$ hr) was increased compared to control ($k = 0.58 \pm 0.1$ hr^{-1}, $t_{1/2} = 1.3$ hr). The total amount (medium+cell+BC) of azacyclonol was significantly greater, while the amount (medium+cell+BC) of generated fexofenadine was similar, at 1, 2, and 4 hr following administration of terfenadine in DEX-treated Day 4 SC rat hepatocytes compared to control (Table 2).

Pharmacokinetic Modeling of Terfenadine and Fexofenadine Disposition in Day 4 SC Rat Hepatocytes. The parameter estimates generated by compartmental modeling of terfenadine, generated fexofenadine, azacyclonol, and preformed fexofenadine data following incubation of terfenadine or preformed fexofenadine in control and DEX-treated Day 4 SC rat hepatocytes are compiled in Table 3. The lines shown in Figure 3 represent the fit of Model 3 to preformed fexofenadine pooled data (n = 3). The lines shown in Figure 4 represent the fit of Model 2 to pooled terfenadine, generated fexofenadine, and azacyclonol data; rate constants determined in Model 1 were fixed, and parameters describing the disposition of generated fexofenadine were estimated according to the scheme displayed in Figure 2.

The rate constant for hepatocyte uptake was faster for terfenadine compared to preformed fexofenadine (2.5 hr^{-1} *vs.* 0.08 hr^{-1}, respectively), while the biliary excretion rate constant for preformed fexofenadine exceeded that of terfenadine (0.44 hr^{-1} vs. 0.039 hr^{-1}, respectively). The rate constant for basolateral excretion of terfenadine and fexofenadine were comparable (3.2 hr^{-1} vs. 1.9 hr^{-1}, respectively). The rate constant for

formation of azacyclonol was greater in DEX-treated Day 4 SC rat hepatocytes (0.76 hr^{-1}) as compared to control cells (0.041 hr^{-1}) (Figure 4; Table 3). While good correspondence of the model to the data was observed, the rate constants associated with the canalicular efflux and the sinusoidal re-uptake of generated fexofenadine were poorly estimated by Model 2 (coefficients of variation > 60%; Table 3). However, the parameter estimates describing the transport processes of generated fexofenadine from Model 2 were similar to parameter estimates describing hepatic transport of preformed fexofenadine estimated from Model 3, and as such, parameter estimates from Models 1 and 3 were used in subsequent simulations based on the assumption that the disposition of preformed fexofenadine and generated fexofenadine was identical.

Simulation of Terfenadine and Generated Fexofenadine Disposition in Day 4 SC Rat Hepatocytes. The disappearance of terfenadine from the incubation (medium+cell+BC) (Figure 6; inset, data points) appeared to be bi-exponential. The disposition of terfenadine in hepatocytes (Model 2; Figure 2) was simulated using the rate constants listed in Table 3; this simulation of the concentration-time profile of terfenadine in medium+cells+BC vs. medium+cells is shown in Figure 6 (inset; solid and dashed lines, respectively). The influence of terfenadine accumulation in the bile canaliculi on the overall loss of terfenadine became more apparent after 4 hr of incubation. Estimates of the rate constants associated with the disposition of terfenadine and fexofenadine in Day 4 control and DEX-treated SC rat hepatocytes (Table 3, bold type) were fixed in Model 2 (Figure 2, Appendix II) to simulate the accumulation of terfenadine and formation of fexofenadine in control and DEX-treated SC rat hepatocytes in cells+BC and cells (Figure 5). In

general, the predicted values of terfenadine and generated fexofenadine were within the standard deviation of the observed data.

Discussion

These experiments represent the first report of an *in vitro* model that can be used to investigate the hepatic uptake, formation, and biliary excretion of a drug/metabolite pair compared with the hepatobiliary disposition of a preformed metabolite. Often, when therapeutic or toxic metabolites are identified in the drug discovery process, they are synthesized and administered to a relevant *in vivo* system in order to identify/confirm beneficial or deleterious effects. However, the disposition of preformed metabolites may not always mimic the disposition of those generated in vivo (Pang et al., 1984). In the case of fexofenadine, for example, a diffusional barrier for hepatic uptake exists for preformed fexofenadine. Although this barrier is not relevant when fexofenadine is generated from terfenadine in the hepatocyte, it could preclude comprehensive evaluation of preformed fexofenadine hepatobiliary disposition in the intact organ.

Following intravenous administration of ^{14}C-TER in rats, approximately 40% and 60% of the total radiolabeled dose was excreted in bile in 4 and 6 hr, respectively, although unchanged terfenadine was not detected in the bile (Leeson et al., 1982). This result suggests that terfenadine metabolism, rather than biliary excretion, is the major route of terfenadine clearance *in vivo* in rats. The disposition of terfenadine and its carboxylate metabolite fexofenadine has been described previously in both *in vivo* and *in vitro* studies. The apparent K_m value for the formation of hydroxyterfenadine (Figure 1) was reported to be ~32 μM in rat liver S9 (Jurima-Romet et al., 1994). Thus, a terfenadine concentration of 5 μM was employed in these studies. The concentration of preformed fexofenadine used in these experiments (5 μM) was chosen based on both the

described K_m values for Oatp1a1 (~32 μM) and Oatp1a4 (~6 μM) (Cvetkovic et al., 1999), and the sensitivity of the HPLC assay.

DEX has been shown to induce transport protein mRNA and protein expression levels in SC rat hepatocytes, including Oatp1a4 to a small extent; DEX did not induce the expression of Oatp1a1 in SC rat hepatocytes (Annaert et al., 2001; Luttringer et al., 2002; Turncliff et al., 2004). DEX treatment (100 μM; 48 hr) of SC rat hepatocytes increased the expression of CYP3A1/2 (Turncliff et al., 2004). Following incubation of terfenadine in Day 4 SC rat hepatocytes, formation of fexofenadine and the N-demethylated metabolite azacyclonol was observed (Figure 4, Table 2); the analysis of hydroxyterfenadine (Figure 1) was not possible due to lack of available standard. Previously, Jurima-Romet et al. (1995) reported that the formation of azacyclonol was increased in DEX-treated primary rat hepatocytes, while the formation of hydroxyterfenadine or fexofenadine was not induced. Similarly, in the present study the amount of fexofenadine formed was not affected by DEX treatment (Table 2), and only a modest increase was observed in the fexofenadine formation rate constant (Table 3). These results are in agreement with previous reports that the formation of fexofenadine in rats does not appear to be mediated specifically by the CYP3A1 isozyme (Jurima-Romet et al., 1995; Jurima-Romet et al., 1996). However, DEX treatment did result in increased terfenadine clearance (Figure 6) consistent with a greater than 10-fold increase in the formation rate constant of azacyclonol in DEX-treated SC rat hepatocytes (Table 3).

The *in vitro* biliary clearance of preformed fexofenadine determined in SC rat hepatocytes was ~6 ml/min/kg (Table 1). When this *in vitro* biliary clearance is scaled to the *in vivo* condition (Liu et al.,1999a), an *in vivo* intrinsic biliary clearance of ~16

ml/min/kg is predicted. The *in vivo* biliary clearance of fexofenadine in Sprague Dawley rats recently was reported to be 11.4 ± 1.6 ml/min/kg (Tahara et al. 2005). Under the assumptions of the well-stirred model of hepatic disposition (Pang and Rowland, 1977), and assuming hepatic blood flow of 40 mL/min (Pollack et al., 1990), the intrinsic biliary clearance of preformed fexofenadine based on the work of Tahara et al. (2005) would be ~ 17 ml/min/kg. Similarly, the intrinsic biliary clearance of preformed fexofenadine in the isolated perfused rat liver would be ~ 20 ml/min/kg (Milne et al., 2000). Thus, our *in vitro* result (~16 ml/min/kg) is in good agreement with reported *in vivo* and *in situ* intrinsic biliary clearance values for fexofenadine.

A stepwise compartmental modeling approach was employed to explore rate-limiting processes in the hepatobiliary disposition of terfenadine, fexofenadine, and azacyclonol in Day 4 SC rat hepatocytes. In control SC rat hepatocytes, the rate constant for terfenadine uptake (2.5 hr^{-1}) was ~30-fold higher than that for fexofenadine (0.08 hr^{-1}), consistent with a diffusional barrier for fexofenadine. Rate constants for terfenadine uptake and egress were ~2-fold greater in DEX-treated SC rat hepatocytes. However, the rate constants for uptake ($k_{TERm\rightarrow c}$) and egress ($k_{TERc\rightarrow m}$) across the basolateral membrane were approximately equal (Table 3), consistent with a predominant diffusional mechanism of TER flux across this membrane. A diffusional process for terfenadine accumulation is consistent with nearly 100% absorption of terfenadine following oral administration in humans (Okerholm et al., 1981).

Rate constants for terfenadine and fexofenadine basolateral efflux in control SC rat hepatocytes were of the same order of magnitude. If a diffusional barrier exists for fexofenadine, but not for terfenadine, the similarity in rate constants for basolateral egress

suggests that fexofenadine excretion across the basolateral membrane is mediated by an active process. The role of Mrps in the basolateral efflux of fexofenadine is the subject of ongoing investigation. The appearance of fexofenadine in fresh HBSS following a 1-hr incubation of terfenadine in Day 4 SC rat hepatocytes provided evidence of basolateral efflux (Figure 4). This observation is consistent with the fact that FEX is excreted in urine following terfenadine administration *in vivo* (Leeson et al., 1982); the sequential processes of terfenadine uptake in the liver, terfenadine metabolism to fexofenadine, and excretion of fexofenadine from the hepatocyte into sinusoidal blood, would be prerequisite to the appearance of fexofenadine in urine.

In a simulation of the cellular accumulation of generated fexofenadine (Figure 5), the parameter estimate for the biliary excretion of preformed fexofenadine adequately described the biliary elimination of generated fexofenadine, indicating that intracellular fexofenadine, at a given concentration, is excreted into bile at the same rate either regardless of whether it is preformed or generated metabolite. Therefore, when diffusional barriers do not limit the access of a metabolite to a clearance mechanism (e.g. biliary excretion), the disposition of the generated metabolibte may mimic that of the preformed administered metabolite.

The rate constant for the biliary excretion of fexofenadine (0.44 hr^{-1})was ~10-fold higher than that for terfenadine (0.039 hr^{-1}), consistent with the extensive biliary excretion of fexofenadine and extensive metabolism compared to terfenadine observed *in vivo* (Leeson et al., 1982). The calculation of BEI (see Methods) is an algebraic approach to estimate the percentage of substrate taken up by hepatocytes that is excreted into bile. The BEI is analogous to the ratio of the biliary excretion rate constant to the sum of rate

constants for excretion of substrate from SC hepatocytes [e.g., $(k_{FEXC\rightarrow B})/(k_{FEXC\rightarrow M} + k_{FEXC\rightarrow B})*100$], where the rate constants are determined based on the compartmental modeling approach. The BEI was similar to the related ratio of rate constants for preformed fexofenadine (19% vs 18%, respectively), but not for terfenadine (15% vs. < 1%, respectively). This overprediction of the biliary excretion of terfenadine in SC rat hepatocytes using the BEI calculation occurs when the molar amount of terfenadine converted to metabolites residing in cells+media+bile is not included in the denominator of the BEI equation. *In vivo*, the metabolism of terfenadine is rapid and parent terfenadine was not detected in the bile of rats administered an intravenous dose (Leeson et al., 1982). Therefore, the BEI and $Cl_{B\ in\ vitro}$ values determined in these experiments may be more representative of the *maximal* values expected *in vivo* for a metabolically labile compound. These observations are consistent with the PK modeling and simulation work of Liu and Pang (2005), who predicted that a decrease in the intrinsic metabolic clearance of enalapril would result in a significant increase in predicted biliary clearance.

The liver is a dynamic organ responsible for the uptake, metabolism, and excretion of many therapeutic agents. While the utility of a double-transport protein transfected cell line to examine the relative rates of transport across the apical and basolateral membranes is apparent (Sasaki et al., 2004), the availability of both transport and metabolism processes in a single experimental system, such as SC hepatocytes, can provide additional insight into the hepatobiliary disposition of novel therapeutic agents. Although a potential limitation of the current model is the decline in metabolic activity during the days in culture required for the transport proteins to become properly localized

for biliary excretion experiments, relevant metabolic function can be maintained by use of media additives such as dexamethasone (LeCluyse et al., 1996; Turncliff et al., 2004). Another consideration is that the tight-junctional complexes which seal the bile canalicular spaces in SC rat hepatocytes can be disrupted continuously by Ca^{2+} modulation only for a limited time (Liu et al., 1999c); thus, accumulation studies to evaluate biliary excretion beyond 1 hr may not be feasible. The SC model may be useful for assessing the overall magnitude of metabolism and/or biliary excretion of novel compounds, as well as to identify species-specific differences in these processes. The use of SC human hepatocytes for prediction of *in vivo* metabolism and biliary excretion is the focus of on-going efforts.

Pharmacokinetic modeling of data from experiments in SC rat hepatocytes can yield the relative rates of hepatobiliary disposition of compounds. These studies represent a robust evaluation of the hepatobiliary disposition of a metabolite when administered preformed vs. when generated by metabolic conversion of a parent compound and emphasize the utility of an *in vitro* model capable of assessing, in an integrated fashion, metabolism, biliary excretion, and basolateral transport processes.

References

Annaert PP, Turncliff RZ, Booth CL, Thakker DR and Brouwer KLR (2001) P-glycoprotein-mediated in vitro biliary excretion in sandwich-cultured rat hepatocytes. *Drug Metab Dispos* **29**:1277-1283.

Coutant JE, Westmark PA, Nardella PA, Walter SM and Okerholm RA (1991) Determination of terfenadine and terfenadine acid metabolite in plasma using solid-phase extraction and high-performance liquid chromatography with fluorescence detection. *J Chromatogr* **570**:139-148.

Cummins CL, Jacobsen W, Christians U, Benet LZ. (2004) CYP3A4-transfected Caco-2 cells as a tool for understanding biochemical absorption barriers: studies with sirolimus and midazolam. *J Pharmacol Exp Ther.* **308**:143-55.

Cvetkovic M, Leake B, Fromm MF, Wilkinson GR and Kim RB (1999) OATP and P-glycoprotein transporters mediate the cellular uptake and excretion of fexofenadine. *Drug Metab Dispos* **27**:866-871.

Hait WN, Gesmonde JF, Murren JR, Yang JM, Chen HX and Reiss M (1993) Terfenadine (Seldane): a new drug for restoring sensitivity to multidrug resistant cancer cells. *Biochem Pharmacol* **45**:401-406.

Hoffmaster KA, Turncliff RZ, LeCluyse EL, Kim RB, Meier PJ, Brouwer KL. (2004) P-glycoprotein expression, localization, and function in sandwich-cultured primary rat and human hepatocytes: relevance to the hepatobiliary disposition of a model opioid peptide. *Pharm Res.* **21**:1294-302.

Johnson BM, Charman WN, Porter CJ. (2003) Application of compartmental modeling to an examination of in vitro intestinal permeability data: assessing the impact of tissue uptake, P-glycoprotein, and CYP3A. *Drug Metab Dispos.* 31:1151-60.

Jurima-Romet M, Crawford K, Cyr T and Inaba T (1994) Terfenadine metabolism in human liver. In vitro inhibition by macrolide antibiotics and azole antifungals. *Drug Metab Dispos* **22**:849-857.

Jurima-Romet M, Casley WL, Neu JM and Huang HS (1995) Induction of CYP3A and associated terfenadine N-dealkylation in rat hepatocytes cocultured with 3T3 cells. *Cell Biol Toxicol* **11**:313-327.

Jurima-Romet M, Huang HS, Beck DJ and Li AP (1996) Evaluation of drug interactions in intact hepatocytes: Inhibitors of terfenadine metabolism. *Toxicology in Vitro* **10**:655-663.

Kostrubsky VE, Strom SC, Hanson J, Urda E, Rose K, Burliegh J, Zocharski P, Cai H, Sinclair JF, Sahi J (2003) Evaluation of hepatotoxic potential of drugs by inhibition of bile-acid transport in cultured primary human hepatocytes and intact rats. *Toxicol Sci.* **76**:220-8.

LeCluyse EL, Audus KL and Hochman JH (1994) Formation of extensive canalicular networks by rat hepatocytes cultured in collagen-sandwich configuration. *Am J Physiol* **266**:C1764-1774.

LeCluyse EL, Bullock PL, Parkinson A and Hochman JH (1996) Cultured rat hepatocytes. *Pharm Biotechnol* **8**:121-159.

Leeson GA, Chan KY, Knapp WC, Biedenbach SA, Wright GJ and Okerholm RA (1982) Metabolic disposition of terfenadine in laboratory animals. *Arzneimittelforschung* **32**:1173-1178.

Li AP and Jurima-Romet M (1997) Applications of primary human hepatocytes in the evaluation of pharmacokinetic drug-drug interactions: evaluation of model drugs terfenadine and rifampin. *Cell Biol Toxicol* **13**:365-374.

Li AP (1997) Primary hepatocyte cultures as an in vitro experimental model for the evaluation of pharmacokinetic drug-drug interactions. *Adv Pharmacol* **43**:103-130.

Liu L and Pang KS (2005) The roles of transporters and enzymes in hepatic drug processing. *Drug Metab Dispos* 33:1-9.

Liu X, Chism JP, LeCluyse EL, Brouwer KR and Brouwer KLR (1999a) Correlation of biliary excretion in sandwich-cultured rat hepatocytes and in vivo in rats. *Drug Metab Dispos* **27**:637-644.

Liu X, LeCluyse EL, Brouwer KR, Gan LS, Lemasters JJ, Stieger B, Meier PJ and Brouwer KLR (1999b) Biliary excretion in primary rat hepatocytes cultured in a collagen-sandwich configuration. *Am J Physiol* **277**:G12-21.

Liu X, LeCluyse EL, Brouwer KR, Lightfoot RM, Lee JI and Brouwer KLR (1999c) Use of Ca2+ modulation to evaluate biliary excretion in sandwich-cultured rat hepatocytes. *J Pharmacol Exp Ther* **289**:1592-1599.

Luttringer O, Theil FP, Lave T, Wernli-Kuratli K, Guentert TW and de Saizieu A (2002) Influence of isolation procedure, extracellular matrix and dexamethasone on the regulation of membrane transporters gene expression in rat hepatocytes. *Biochem Pharmacol* **64**:1637-1650.

Milne RW, Larsen LA, Jorgensen KL, Bastlund J, Stretch GR and Evans AM (2000) Hepatic disposition of fexofenadine: influence of the transport inhibitors erythromycin and dibromosulphothalein. *Pharm Res* **17**:1511-1515.

Mizuno N, Niwa T, Yotsumoto Y, Sugiyama Y. (2003) Impact of drug transporter studies on drug discovery and development. *Pharmacol Rev.* 55:425-61.

Okerholm RA, Wiener DL, Hook RH, Walker BJ, Leeson GA, Biedenbach SA, Cawein MJ, Dusebout TD, Wright GJ, Myers M, Schindler V, Cook CE. (1981) Bioavailability of terfenadine in man. *Biopharm Drug Dispos* **2**:185-190

Pang KS and Rowland M (1977) Hepatic clearance of drugs. I. Theoretical considerations of a "well-stirred" model and a "parallel tube" model. Influence of hepatic blood flow, plasma and blood cell binding, and the hepatocellular enzymatic activity on hepatic drug clearance. *J Pharmacokinet Biopharm* **5**:625-653.

Pang KS, Cherry WF, Terrell JA, Ulm EH. (1984) Disposition of enalapril and its diacid metabolite, enalaprilat, in a perfused rat liver preparation. Presence of a diffusional barrier for enalaprilat into hepatocytes. *Drug Metab Dispos.* 12:309-313.

Pollack GM, Brouwer KL, Demby KB, Jones (1990) JA.Determination of hepatic blood flow in the rat using sequential infusions of indocyanine green or galactose. *Drug Metab Dispos.* 18:197-202.

Raeissi SD, Hidalgo IJ, Segura-Aguilar J and Artursson P (1999) Interplay between CYP3A-mediated metabolism and polarized efflux of terfenadine and its metabolites in intestinal epithelial Caco-2 (TC7) cell monolayers. *Pharm Res* **16**:625-632.

Sasaki M, Suzuki H, Aoki J, Ito K, Meier PJ, Sugiyama Y. (2004) Prediction of in vivo biliary clearance from the in vitro transcellular transport of organic anions across a double-transfected Madin-Darby canine kidney II monolayer expressing both rat organic anion transporting polypeptide 4 and multidrug resistance associated protein 2. *Mol Pharmacol.* 66:450-9.

Seglen PO (1976) Preparation of isolated rat liver cells, in *Methods in Cell Biology* 13th ed. (Prescott DM ed) pp 29-83, Academic Press, New York.

Tahara H, Kusuhara H, Fuse E, Sugiyama Y. (2005) P-glycoprotein plays a major role in the efflux of fexofenadine in the small intestine and blood-brain barrier, but only a limited role in its biliary excretion. *Drug Metab Dispos.* **33**:963-968.

Tirona RG, Pang KS. (1996) Sequestered endoplasmic reticulum space for sequential metabolism of salicylamide. Coupling of hydroxylation and glucuronidation. *Drug Metab Dispos.* 24:821-33.

Turncliff RZ, Meier PJ, Brouwer KL (2004) Effect of dexamethasone treatment on the expression and function of transport proteins in sandwich-cultured rat hepatocytes. *Drug Metab Dispos*. 32:834-9.

Wrighton SA, Ring BJ, VandenBranden M. (1995) The use of in vitro metabolism techniques in the planning and interpretation of drug safety studies. *Toxicol Pathol.* 23:199-208.

Yun CH, Okerholm RA and Guengerich FP (1993) Oxidation of the antihistaminic drug terfenadine in human liver microsomes. Role of cytochrome P-450 3A(4) in N-dealkylation and C-hydroxylation. *Drug Metab Dispos* **21**:403-409.

Footnotes.

This research was supported by:

Pfizer Global Research and Development.

National Institutes of Health Grant RO1 GM41935

Figure 1. Scheme of metabolic pathways of terfenadine.

Figure 2. Model schemes depicting the disposition of terfenadine (TER), generated fexofenadine (FEX_{gen}), azacyclonol (AZA) and preformed fexofenadine (FEX_{pre}) in the incubation medium (**M**), hepatocyte (**C**), bile canaliculi (**B**), or total homogenate (**T**; media+cells+BC) of Day 4 SC rat hepatocytes. Italicized rate constants were set to values estimated in Model 1. Biliary excretion rate constants were estimated by simultaneous modeling of accumulation data in cells+BC (shaded compartments represent BC) and cells.

Figure 3. Accumulation of preformed fexofenadine (FEX_{pre}) in control (A) and DEX-treated (B) Day 4 SC rat hepatocytes in Cells+BC (▲) or Cells (∆). Data represent mean ± SEM (n = 3). Solid and dashed lines represent the computer-generated best fit of the equations (Appendix II) describing the compartmental Model 3 (Figure 2) to the data.

Figure 4. Disposition of terfenadine (TER; squares) and generated fexofenadine (FEX_{gen}; triangles) in the incubation medium (closed symbols) and hepatocytes (cells+BC; open symbols), and total azacyclonol (AZA; diamonds; medium+cells+BC) in Control (A) and DEX-treated (B) Day 4 SC rat hepatocytes . Data represent mean ± SEM (n = 3). Lines (solid and dashed) represent the computer-generated best fit of the data to model scheme 2 (Figure 2) and equations described in Appendix II.

Figure 5. Accumulation of terfenadine (TER) (■) and generated fexofenadine (FEX_{gen}) (▲) in control (**A**) or DEX-treated (**B**) Day 4 SC rat hepatocytes incubated with 5 μM terfenadine in cells+BC (closed symbols) or cells (open symbols). Data represent mean ± SEM (n = 3; where not visible, error bars are contained within the symbol). Solid and dashed lines represent computer-simulations of the compartmental Model scheme 2 (Figure 2), using pooled rate constants listed in Table 3 and equations described in Appendix II. Rate constants derived for preformed fexofenadine (Figure 2, Model 3; Figure 3; Table 3) were used to simulate the accumulation of generated fexofenadine in SC rat hepatocytes in (cells+BC *vs.* cells).

Figure 6. Time course of the disappearance of terfenadine (5 μM) from control (■) and DEX-treated (●) Day 4 SC rat hepatocytes (medium+cells+BC). Data represent mean ± SEM (n = 3). Solid lines represent first-order elimination from a one-compartment model. **Inset:** Time course of the disappearance of terfenadine (5 μM) from control Day 4 SC rat hepatocytes (medium+cells+BC). Lines represent simulations of the compartmental model scheme 2 (Figure 2) in cells+BC (solid line) and cells (dashed line), respectively, using rate constants listed in Table 3 and equations described in Appendix II. The apparent bi-exponential decay of terfenadine is representative of accumulation in the bile canaliculi of Day 4 SC rat hepatocytes; terfenadine loss from cells (in the absence of bile canaliculi) was monoexponential (dashed line).

JPET Fast Forward. Published on May 11, 2006 as DOI: 10.1124/jpet.106.102616
This article has not been copyedited and formatted. The final version may differ from this version.

Table 1. Comparison of BEI and $Cl_{B\,in\ vitro}$ values of terfenadine (TER), generated fexofendine (FEX) and preformed fexofenadine between control and DEX-treated (100 μM, 48 hr) Day 4 SC rat hepatocytes. Data represent mean ± SEM of three individual experiments performed in triplicate.

	BEI[1] (%)		$Cl_{B\ in\ vitro}$[2] (ml/min/kg)	
	Control	Treated	Control	Treated
TER	15 ± 4*	9 ± 5	29 ± 10	20 ± 7
Generated FEX	15 ± 2	12 ± 4	-	-
Preformed FEX	19 ± 2	20 ± 5	5.9 ± 2.0	4.0 ± 0.9

[1] Biliary excretion index (BEI) values (1 hr) were calculated as described in the Methods section.
[2] *In vitro* biliary clearance ($Cl_{B\,in\ vitro}$) values (1 hr) were calculated according to equations in the Appendix I
* $p < 0.05$ vs. Treated.

Table 2. Disposition of terfenadine in Control and DEX-treated (100 μM; 48 hr) Day 4 SC rat hepatocytes. Amount (nmol) of terfenadine and the metabolites fexofenadine and azacyclonol in medium and hepatocytes (cells+BC) following incubation of terfenadine (5 μM). Data represent mean ± S.D. of three individual experiments.

	Control							
Time	TER (nmol)		FEX (nmol)		AZA (nmol)		(nmol)	Recovery
(hr)	Medium	Cell + Bile	Medium	Cell + Bile	Medium	Cell + Bile	Total	(%)
1	5.6 ± 1.6	3.7 ± 0.3	1.0 ± 0.4	1.5 ± 0.5	0.16 ± 0.08	0.15 ± 0.05	12 ± 3	81 ± 18
2	3.6 ± 0.7*	2.1 ± 0.9	2.8 ± 0.7*	1.6 ± 0.2	0.21 ± 0.09	0.15 ± 0.02	10 ± 0.9	64 ± 6
4	0.5 ± 0.1*	1.6 ± 0.6	5.6 ± 0.8*	1.3 ± 0.2	0.22 ± 0.07	0.11 ± 0.03	10 ± 0.1	67 ± 7
	DEX-Treated							
Time	TER (nmol)		FEX (nmol)		AZA (nmol)		(nmol)	Recovery
(hr)	Medium	Cell + Bile	Medium	Cell + Bile	Medium	Cell + Bile	Total	(%)
1	3.1 ± 0.4†	2.1 ± 0.3†	1.8 ± 0.4	1.3 ± 0.3	1.1 ± 0.04†	1.3 ± 0.3†	10 ± 2	73 ± 15
2	1.1 ± 0.0*†	1.1 ± 0.2	4.5 ± 0.7†	0.8 ± 0.1†	1.6 ± 0.2†	2.2 ± 0.7†	11 ± 2	74 ± 13
4	<LLOQ	0.3 ± 0.1	6.5 ± 0.7†	0.6 ± 0.1*†	2.3 ± 0.3*†	1.3 ± 0.0†	11 ± 2	74 ± 12

<LLOQ: Below the lower limit of quantitation

* $p < 0.05$ *vs.* 1 hour (same treatment); † $p < 0.05$ *vs.* control (same timepoint)

JPET Fast Forward. Published on May 11, 2006 as DOI: 10.1124/jpet.106.102616
This article has not been copyedited and formatted. The final version may differ from this version.

Table 3. Kinetic parameters (hr^{-1}) associated with the disposition of terfenadine and preformed fexofenadine in control and DEX-treated SC rat hepatocytes. Terfenadine (5 μM) and preformed fexofenadine (5 μM) were incubated with Day 4 SC rat hepatocytes as described in the methods. Parameter estimates were generated by non-linear regression of the pooled data based on the equations described in Appendix II according to the model schemes shown in Figure 2. Bold type: fixed parameter estimates used in simulation experiment (Figure 5).

		Control		Treated	
	Parameter	Estimate	CV (%)	Estimate	CV (%)
Model 1 (TER - FEX_{TOT})	$k_{TER_M \rightarrow TER_C}$	**2.5**	*7*	**6.4**	*10*
	$k_{TER_C \rightarrow TER_M}$	**3.2**	*12*	**8.8**	*8*
	$k_{TER_C \rightarrow TER_B}$	**0.039**	*48*	**0.048**	*37*
	$k_{TER_C \rightarrow FEX_T}$	**0.67**	*7*	**1.2**	*7*
	$k_{TER_C \rightarrow AZA_T}$	**0.041**	*95*	**0.76**	*10*
	$k_{TER_C \rightarrow Other}$	**0.86**	*8*	**0.86**	*8*
Model 3 (Preformed FEX)	$k_{FEX_M \rightarrow FEX_C}$	**0.080**	*3*	**0.065**	*6*
	$k_{FEX_C \rightarrow FEX_M}$	**1.9**	*5*	**2.5**	*11*
	$k_{FEX_C \rightarrow FEX_B}$	**0.44**	*7*	**0.45**	*16*
Model 2 (Generated FEX)	$k_{FEX_M \rightarrow FEX_C}$	0.089	*61*	0.069	*98*
	$k_{FEX_C \rightarrow FEX_M}$	1.5	*17*	2.0	*18*
	$k_{FEX_C \rightarrow FEX_B}$	0.44	*>100*	0.45	*>100*

Subscripts: M = media, C = cell, B = bile canaliculi, T = total (M+C+B)

Figure 1

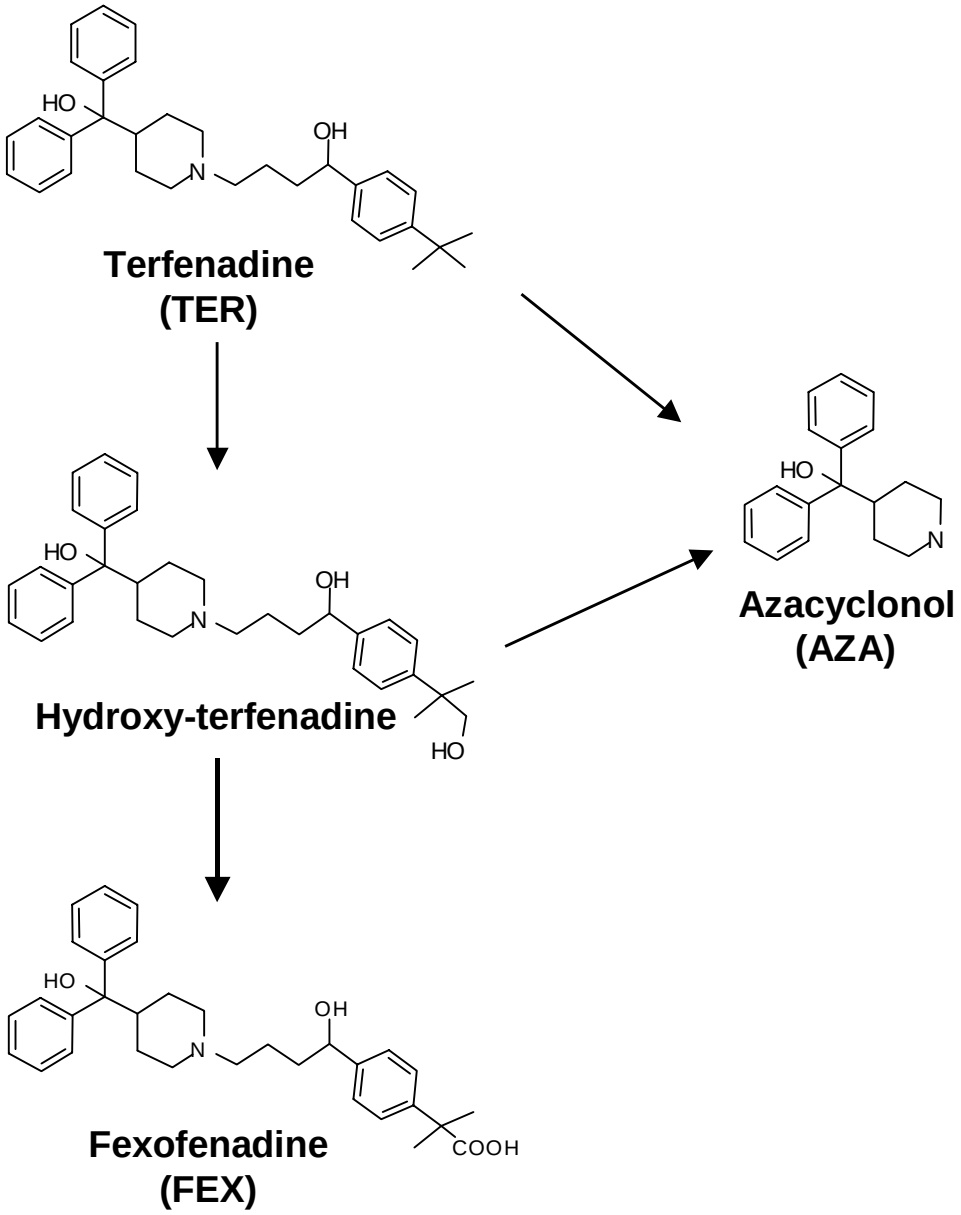

Figure 2

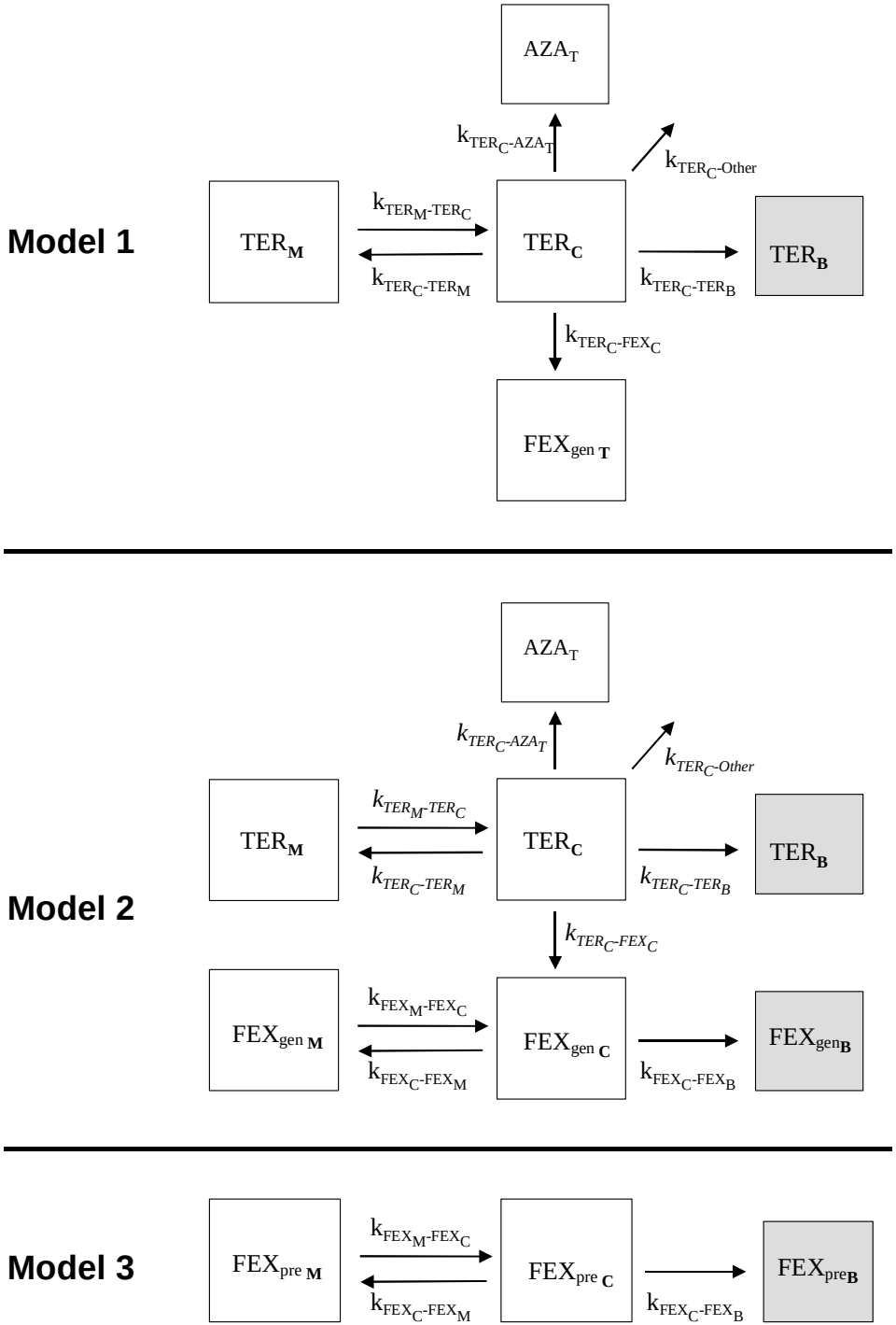

Figure 3

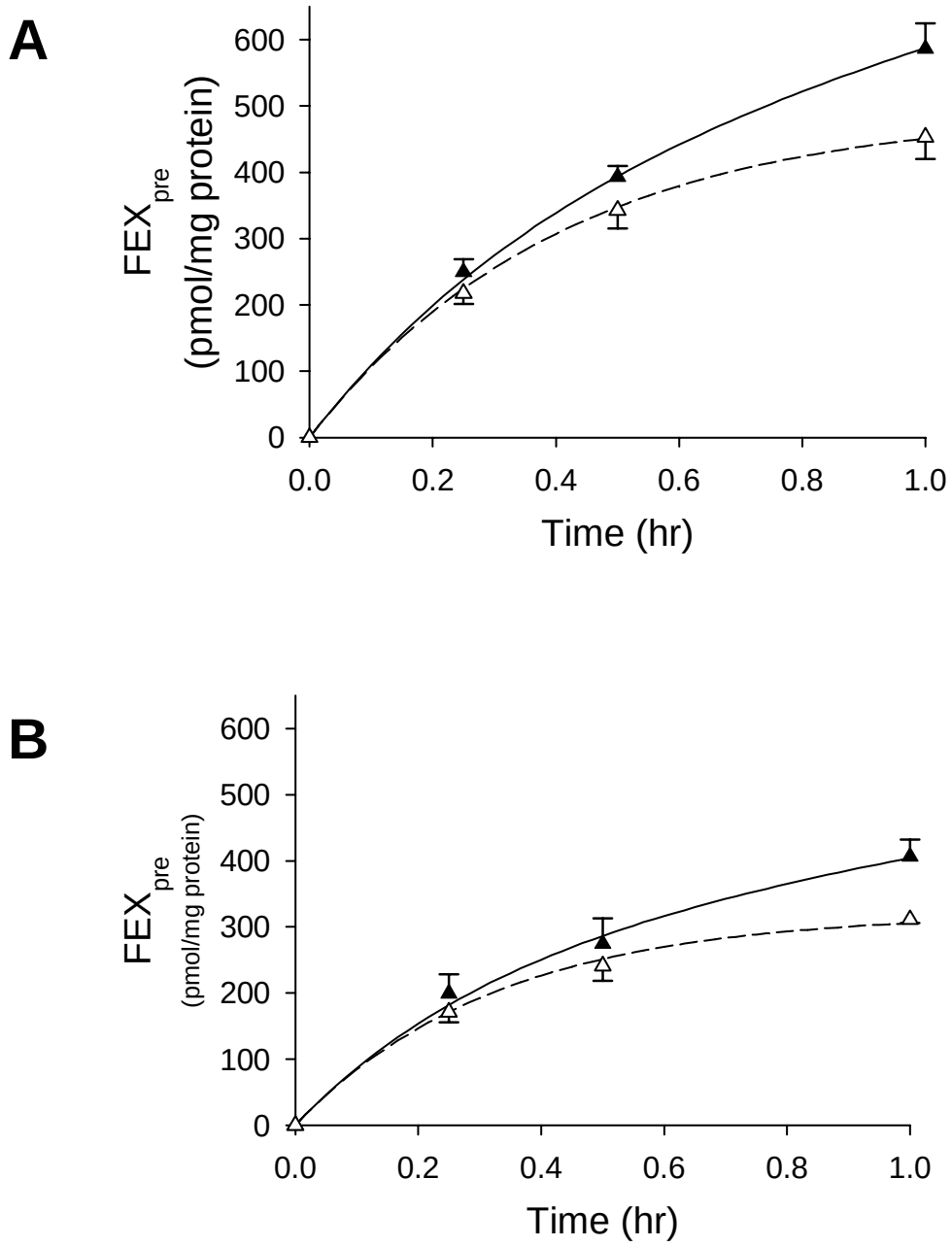

Figure 4

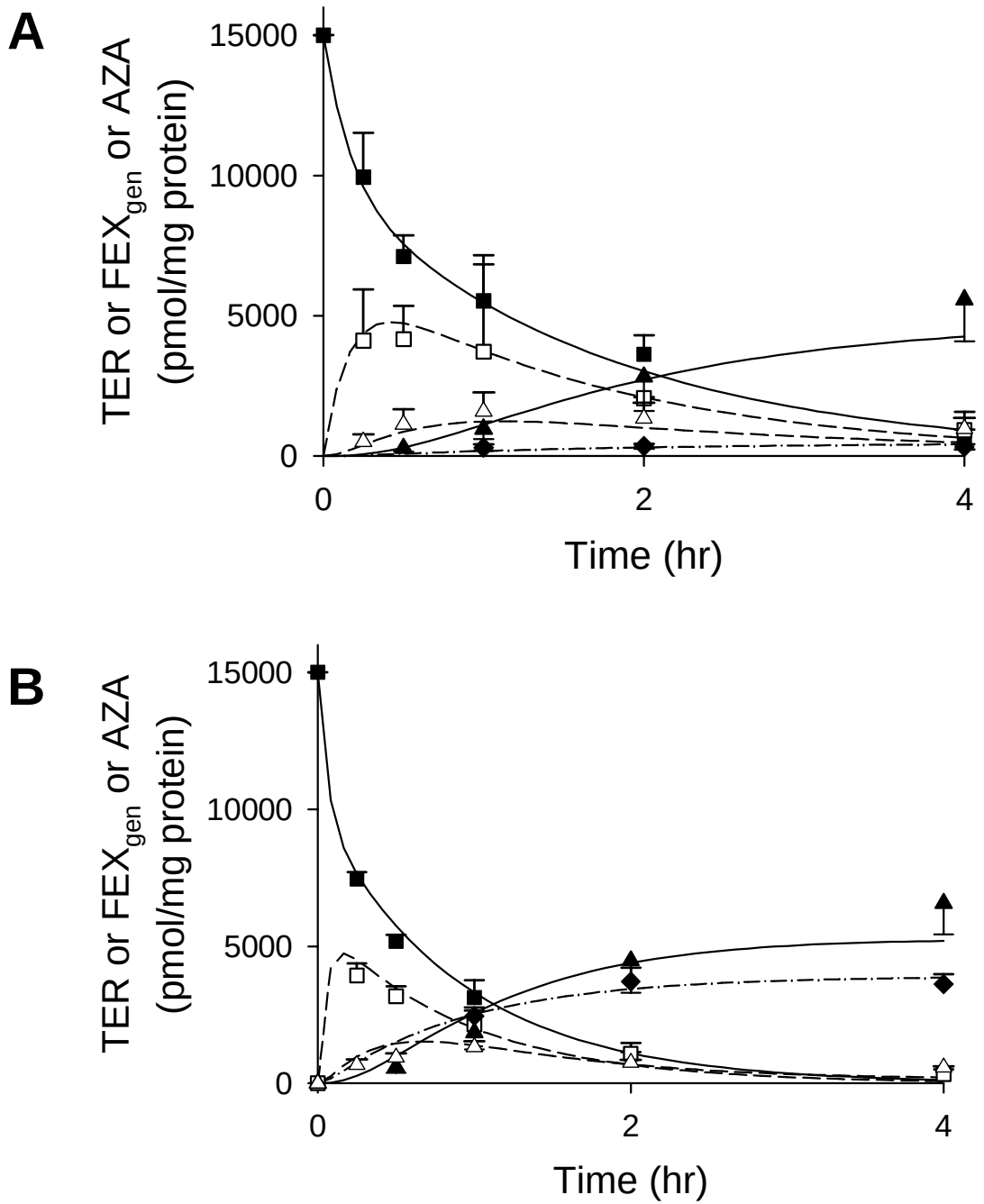

Figure 5

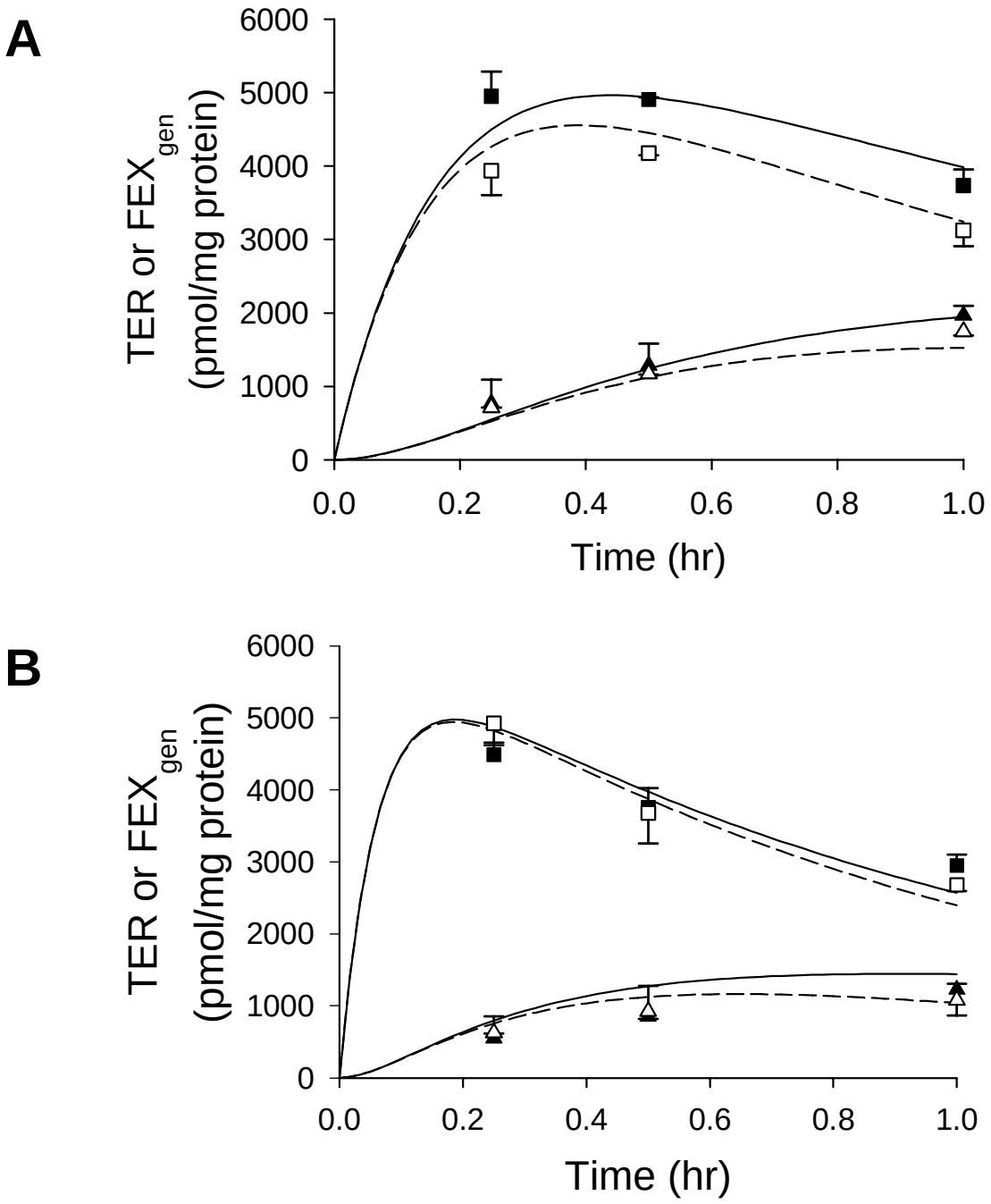

Figure 6

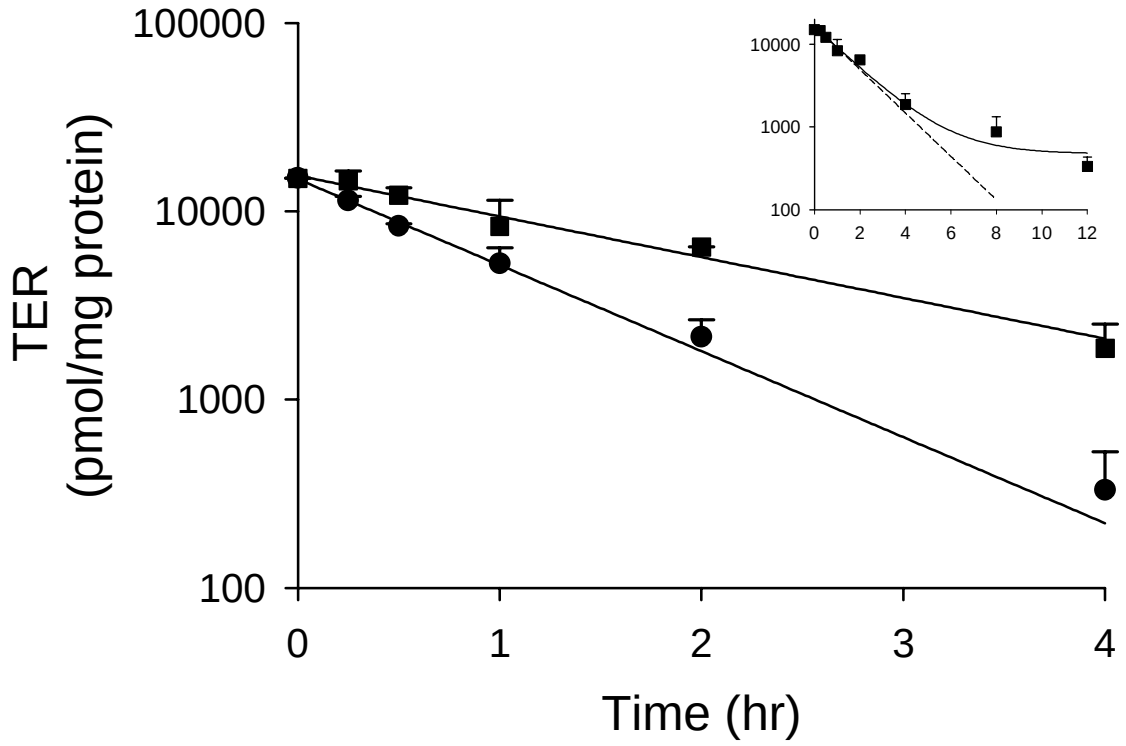

JPET Fast Forward. Published on May 11, 2006 as DOI: 10.1124/jpet.106.102616
This article has not been copyedited and formatted. The final version may differ from this version.

APPENDIX I

Calculation of *in vitro* Biliary Clearance

The *in vitro* biliary clearance values of preformed fexofenadine (FEX_{pre}), terfenadine (TER) and generated fexofenadine (FEX_{gen}) in Table 2 were calculated according to equations 1 and 2 below. Rat liver weight and protein content in liver tissue were assumed to be 40 g/kg body weight and 0.2 g/g liver weight, respectively, in all calculations (Seglen, 1976).

KEY: M = Media; C = Cell; B = Bile; Accum = total accumulation of substrate under stated condition.

Calculation of preformed FEX $Cl_{B\ in\ vitro}$:

$$Cl_{B\ in\ vitro\ \boldsymbol{FEXpre}} = \frac{\text{Accum } FEX_{pre\ Cells + BC} - \text{Accum } FEX_{pre\ Cells}}{AUC_{0\text{-}60\ FEX_{pre}}} \qquad \mathbf{1}$$

$$AUC_{0\text{-}60\ FEX_{pre}} = \text{Time} * \text{Concentration}_{FEXpre\ \mathbf{M}}$$

where $\text{Concentration}_{FEXpre}$ in the incubation medium was unchanged (5 μM) (data not shown): $AUC_{0\text{-}60FEXpre}$ = 300 nmol*min/ml (Control and Treated)

Calculation of TER $Cl_{B\ in\ vitro}$:

$$Cl_{B\ in\ vitro\ \boldsymbol{TER}} = \frac{\text{Accum TER}_{Cells + BC} - \text{Accum TER}_{Cells}}{AUC_{0\text{-}60\ TER\ \mathbf{M}}} \qquad \mathbf{2}$$

$AUC_{0\text{-}60TER\ \mathbf{M}}$ = 167 nmol*min/ml (Control) or 126 nmol*min/ml (Treated); calculated using the log trapezoidal method using data shown in Figure 4.

JPET Fast Forward. Published on May 11, 2006 as DOI: 10.1124/jpet.106.102616
This article has not been copyedited and formatted. The final version may differ from this version.

APPENDIX II

Equations describing the metabolic and biliary disposition of TER, generated FEX, preformed FEX, and AZA in Day 4 SC rat hepatocytes.

The following equations, based on model schemes shown in Figure 2, were used in the step-wise regression analysis of observed data. Parameter estimates of the transport and metabolic processes responsible for the hepatobiliary disposition of TER and FEX and AZA are described in Table 3. The following abbreviations and subscripts are used: TER, terfenadine; FEX_{pre}, preformed fexofenadine; FEX_{gen}, generated fexofenadine; AZA, azacyclonol; M, incubation medium; C, cellular; B, canalicular network; T, total (M+C+B). All data were modeled as amounts (pmol/mg protein).

Model 1

$$\frac{dTER_M}{dt} = -k_{TER_M\text{-}TER_C} * TER_M + k_{TER_C\text{-}TER_M} * TER_C \quad \textbf{3}$$

$$\frac{dTER_C}{dt} = k_{TER_M\text{-}TER_C} * TER_M - (k_{TER_C\text{-}TER_M} + k_{TER_C\text{-}AZA_T} + k_{TER_C\text{-}Other} + k_{TER_C\text{-}TER_B} + k_{TER_C\text{-}FEX_C}) * TER_C \quad \textbf{4}$$

$$\frac{dTER_B}{dt} = k_{TER_C\text{-}TER_B} * TER_C \quad \textbf{5}$$

$$\frac{dAZA_T}{dt} = k_{TER_C\text{-}AZA_T} * TER_C \quad \textbf{6}$$

$$\frac{dFEX_{genT}}{dt} = k_{TER_C\text{-}FEX_C} * TER_C \quad \textbf{7}$$

JPET Fast Forward. Published on May 11, 2006 as DOI: 10.1124/jpet.106.102616
This article has not been copyedited and formatted. The final version may differ from this version.

Model 2

Accumulation in Cells+BC: Equations 3-6. Additionally:

$$\frac{d\mathrm{FEX}_{\mathrm{genC}}}{d\mathrm{t}} = k_{\mathrm{TER_C\text{-}FEX_C}} * \mathrm{TER_C} + k_{\mathrm{FEX_M\text{-}FEX_C}} * \mathrm{FEX_{genM}} - (k_{\mathrm{FEX_C\text{-}FEX_M}} + k_{\mathrm{FEX_C\text{-}FEX_B}}) * \mathrm{FEX_{genC}} \quad \textbf{8}$$

$$\frac{d\mathrm{FEX}_{\mathrm{genM}}}{d\mathrm{t}} = - k_{\mathrm{FEX_M\text{-}FEX_C}} * \mathrm{FEX_{genM}} + k_{\mathrm{FEX_C\text{-}FEX_M}} * \mathrm{FEX_{genC}} \quad \textbf{9}$$

$$\frac{d\mathrm{FEX}_{\mathrm{genB}}}{d\mathrm{t}} = k_{\mathrm{FEX_C\text{-}FEX_B}} * \mathrm{FEX_{genC}} \quad \textbf{10}$$

Accumulation in Cells: Equations 4, 6, and 8. Additionally:

$$\frac{d\mathrm{TER}_{\mathrm{M}}}{d\mathrm{t}} = -k_{\mathrm{TER_M\text{-}TER_C}} * \mathrm{TER_M} + (k_{\mathrm{TER_C\text{-}TER_M}} + k_{\mathrm{TER_C\text{-}TER_B}}) * \mathrm{TER_C} \quad \textbf{11}$$

$$\frac{d\mathrm{FEX}_{\mathrm{genM}}}{d\mathrm{t}} = - k_{\mathrm{FEX_M\text{-}FEX_C}} * \mathrm{FEX_{genM}} + (k_{\mathrm{FEX_C\text{-}FEX_M}} + k_{\mathrm{FEX_C\text{-}FEX_B}}) * \mathrm{FEX_{genC}} \quad \textbf{12}$$

Model 3

Accumulation in Cells+BC:

$$\frac{d\mathrm{FEX}_{\mathrm{preM}}}{d\mathrm{t}} = - k_{\mathrm{FEX_M\text{-}FEX_C}} * \mathrm{FEX_{preM}} + k_{\mathrm{FEX_C\text{-}FEX_M}} * \mathrm{FEX_{preC}} \quad \textbf{13}$$

$$\frac{d\mathrm{FEX}_{\mathrm{preC}}}{d\mathrm{t}} = k_{\mathrm{FEX_M\text{-}FEX_C}} * \mathrm{FEX_{preM}} - (k_{\mathrm{FEX_C\text{-}FEX_M}} + k_{\mathrm{FEX_C\text{-}FEX_B}}) * \mathrm{FEX_{preC}} \quad \textbf{14}$$

$$\frac{d\mathrm{FEX}_{\mathrm{preB}}}{d\mathrm{t}} = k_{\mathrm{FEX_C\text{-}FEX_B}} * \mathrm{FEX_{preC}} \quad \textbf{15}$$

Accumulation in Cells: Equation 14. Additionally:

$$\frac{d\mathrm{FEX}_{\mathrm{preM}}}{d\mathrm{t}} = - k_{\mathrm{FEX_M\text{-}FEX_C}} * \mathrm{FEX_{preM}} + (k_{\mathrm{FEX_C\text{-}FEX_M}} + k_{\mathrm{FEX_C\text{-}FEX_B}}) * \mathrm{FEX_{preC}} \quad \textbf{16}$$